

Review

Bridging the Gap between Reality and Ideality of Graphdiyne: The Advances of Synthetic Methodology

Ya Kong,^{1,3} Jiaqiang Li,^{1,3} Sha Zeng,¹ Chen Yin,^{1,2} Lianming Tong,¹ and Jin Zhang^{1,*}

Recently, various synthetic methods have been developed to synthesize graphdiyne (GDY) in the aspect of controlled layer and different morphologies. The ideal GDY should have a large crystal domain size with only one atomic layer and possess excellent mechanical, electronic, optical, and magnetic intrinsic properties. However, there is still a gap between the reality and ideality on the road to perfect GDY, which results from the synthetic challenges from the terminal alkynes coupling efficiencies, side reactions, free rotation of carbon-carbon single bond between the diacetylenic linkages, small domain size, defects, and the uncontrollability of thickness. In this review, we will summarize the advances of synthetic methodology in improving the quality and yield of GDY from the perspective of fundamental acetylenic coupling reactions. We aim to stimulate the interest of researchers working in controlled synthesis and broaden application fields of GDY.

INTRODUCTION

Graphdiyne (GDY) is a kind of two-dimensional (2D) all-carbon nanomaterial with specific configuration of sp and sp² hybridized carbon atoms. Thanks to the unique structures of diacetylenic linkages (–C≡C–C≡C–), large π-conjugated systems, and well-distributed pores, GDY presents remarkable potential applications in the fields of energy storage and transformation,^{1–4} catalysis,^{5–9} gas separation,^{10,11} biomedicine,¹² etc. Monolayer GDY is predicted to be a 2D semiconductor with a moderate band gap of 0.44–1.47 eV based on different calculation methods^{3,10,13–18} and an intrinsic carrier mobility of 10⁴–10⁵ cm²·V^{–1}·s^{–1} at room temperature,¹³ making it an outstanding 2D material for future electronic, optoelectronic, and spintronic applications.¹⁹

Since GDY was first proposed by Haley in 1997, it has been predicted to be the most stable artificial carbon allotrope with heat formation of 18.3 kcal per g-atom C.²⁰ Therefore, the architecture of GDY is the direction for many scientists' efforts. Considering the unique structure and properties, much effort has been devoted to exploring the synthetic methods of single or few-layered GDY.^{21–23} In 2010, Li and co-workers reported the first laboratory fabrication of GDY films on copper foils using an *in situ* Glaser coupling reaction.²⁴ Mao's group also proposed an approach of aqueous phase exfoliation to obtain damage-free and few-layered GDY with high yields.²⁵ In the past decade, a variety of approaches have been developed to synthesize GDY with controllable layer and different morphologies, such as GDY films,^{21–27} nanowalls,^{28,29} nanoribbons,³⁰ nanosheets,^{22,31} nanotubes,³² and freestanding three-dimensional (3D) GDY.³³

Despite tremendous progress in the synthesis of highly ordered GDY, there is a gap between reality and ideality due to some intrinsic synthetic problems and challenges

The Bigger Picture

Carbon nanomaterials have drawn great attention in recent years because of their outstanding properties and widespread applications. Graphdiyne (GDY) is a two-dimensional carbon nanomaterial consisting of sp and sp² hybridized carbon atoms. Because of the unique structure and advanced physical and chemical properties, GDY exhibits extensive potential applications in many fields, such as catalysis, electrochemical energy storage, optoelectronic devices, and biomedicine. Similar to any material, synthesis determines the future. In order to bridge the gap between reality and ideality of GDY, many methods have been developed. However, until now, there has been a lack of fully deep summarizations, analyses, and prospects regarding the synthetic methodology of GDY. Hence, we will focus on the GDY synthetic methodology in the aspect of basic acetylenic coupling reactions, controllable synthetic methods, and scale-up production. This review will give important guidance on the synthesis of GDY.

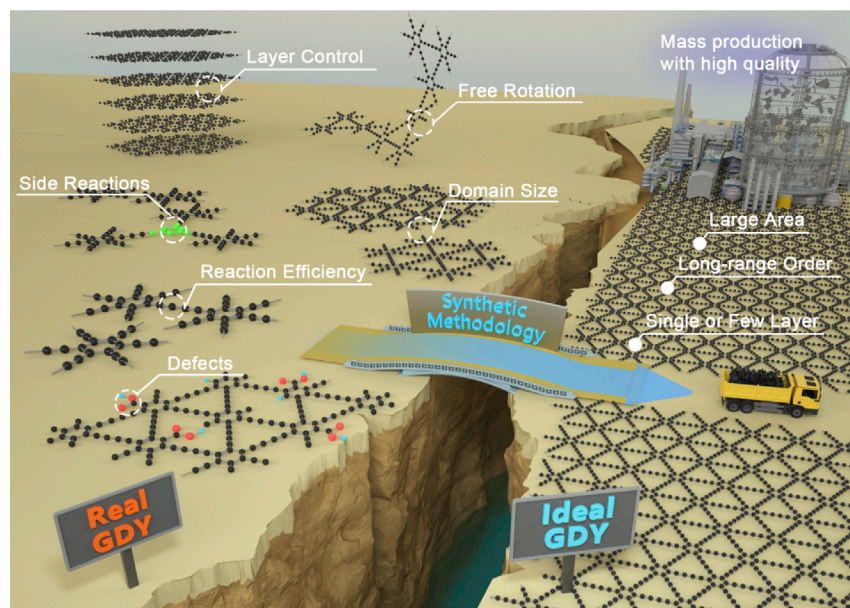


Figure 1. Schematic Illustration of the Gap between Reality and Ideality of GDY

Black ball and green ball, carbon atom; red ball, oxygen atom; blue ball, hydrogen atom.

(Figure 1).³⁴ As mentioned above, the ideal GDY should have a large crystal domain with one atomic layer and possess excellent mechanical, electronic, optical, and magnetic properties.^{35,36} Nevertheless, the performances of as-synthesized GDY are not the same as the theoretical prediction, due to the polycrystalline or amorphous nature of GDY. Therefore, the preparation of ideal GDY, especially the single crystal monolayered GDY, is an urgent issue. In 2009, Sakamoto et al. discussed the synthetic approaches and issues of GDY-based 2D polymers.³⁷ The unprotected terminal alkyne compounds with high chemical sensitivity are considered as a disadvantage to the ideal GDY. In the process of reactions, because of the multiple intramolecular cyclization and numerous bonds that should be formed at the right place, the number of bond-formations may be limited for hexaethynylbenzene (HEB). Besides, the flexibility of the main skeleton could lead to a 3D geometry in the growth steps. In this respect, a number of challenges are worthwhile mentioned combining theories and experiments: (1) the terminal alkyne coupling efficiencies of monomer, HEB, are difficult to be equivalent to coupling reaction of phenylacetylene under the same reaction conditions; (2) the side reactions, such as oxidative addition, cyclotrimerization, and reductive elimination coupling reactions, appear and affect crystallinity of GDY because of the high activity of the monomers;³⁸ (3) the free rotation of carbon-carbon single bond between the diacetylenic linkages lead to unordered structure;³⁷ (4) small domain size and defects influence the properties of GDY; and (5) the thickness is difficult to be controlled because of the interaction between GDY layers. The differences between “real GDY” and “ideal GDY” lead to the gap. In order to bridge the gap, rational design of synthetic methods could be an efficient solution.

Recently, there have been comprehensive reviews on the intrinsic properties, synthesis, functionalization, and potential applications of GDY.^{4,6,12,34–36,39,40} Nevertheless, the challenges from the point of view of synthetic methodology of GDY have not been fully addressed. Deep reviews about how to bridge the gap between “real GDY” and “ideal GDY” are scarce. In this review, we will overview the advances of synthetic methodology

¹Center for Nanochemistry, Beijing Science and Engineering Center for Nanocarbons, Beijing National Laboratory for Molecular Sciences, College of Chemistry and Molecular Engineering, Peking University, Beijing 100871, P.R. China

²Academy for Advanced Interdisciplinary Studies, Peking University, Beijing 100871, P.R. China

³These authors contributed equally

*Correspondence: jinzhang@pku.edu.cn
<https://doi.org/10.1016/j.chempr.2020.06.011>

in improving the quality and yield of GDY from the perspective of fundamental acetylenic coupling reactions. Glaser coupling catalyzed by Cu(I) was proposed first, and the subsequent three coupling reactions modified the catalyst systems. In the Glaser-Hay coupling reaction, an organic base was added to improve solubility of the Cu catalyst complex. Cu(II) acetate was applied to the Eglinton coupling reaction, which was carried out by a radical mechanism at room temperature. The utilization of alkynylsilane precursor could improve the stability of monomers in the alkynylsilane reaction. In addition, we highlight several strategies in wet chemical route, including catalyst, monomer, and interface-confined synthetic methods. Subsequently, we give in-depth insights into large-scale synthetic methods of highly ordered GDY by controlling the surface area of substrate, utilizing the solid-liquid interface, and employing graphene as an epitaxy template. Finally, we put forward the prospects for future developments in the synthesis and applications of GDY. We hope that this review would provide an overall analysis of challenges regarding the developed synthetic methods and guide the researchers toward issues that should be taken into consideration in future synthesis of GDY.

FUNDAMENTAL COPPER-MEDIATED ACETYLENIC COUPLING REACTIONS FOR GDY

GDY is a kind of polymeric network comprising sp and sp² hybridized carbon atoms. Hence, the synthesis of GDY could be inspired from the organic molecules as building blocks that connect with each other via chemical bonds. GDY would be realized through the chemical reactions of appropriate precursors theoretically. As proposed by Haley et al., GDY substructures were realized via Cu-mediated acetylenic coupling reactions based on terminal alkynes or their derivatives.^{20,41,42} For conjugated alkynyl groups, Pb-catalyzed Sonogashira coupling reaction based on alkynyl halides could be applied,⁴³ and the controlled oligotrimerization of cyclic polyynes would also lead to the macromolecular networks for GDY.⁴⁴ Whereas, more stable precursors and more valid catalyst systems make Cu-mediated acetylenic coupling reactions stand out as more promising approaches for GDY's synthesis. Until now, four types of Cu-mediated coupling reactions, including Glaser coupling, Glaser-Hay coupling, Eglinton coupling, and alkynylsilane coupling, were conventionally applied in the fabrication of GDY, as concluded in Figure 2A. Understanding of the fundamental catalytic systems and mechanisms of the coupling reactions is critical for developing high-efficient coupling approaches for GDY.

Glaser Coupling Reaction

The observation of acetylenic coupling reaction and that phenylacetylene catalyzed by Cu(I) salt in the alkaline solvent underwent the formation of Cu(I) phenylacetyl intermediate and subsequent oxidative dimerization was first reported by Glaser.⁴⁵ Mechanisms for the classical acetylenic coupling reactions are demonstrated in Figure 2B. As for the Glaser coupling, a speculation of dinuclear-copper-acetylde-complex-mediated oxidized coupling mechanism proposed by Bohlmann et al. was widely accepted.^{46,47} While the monomer of phenylacetylene was utilized in the Glaser coupling, its conversion and yield could reach more than 90%, indicating a high selectivity.⁴⁸ Aiming at the synthesis of stable GDY networks, Li and co-workers designed HEB as the monomer and carried out a modified *in situ* Glaser coupling reaction in the alkaline pyridine solvent.²⁴ They exploited the Cu foil as both the catalyst and planar substrate tactfully since Cu would be oxidized to copper ions in the presence of a basic solvent. The planar Cu surface plays an important catalytic role in the polymerization and drives the synthesis of flat GDY films. Referring to this designing concept, GDY nanotubes³² and strip arrays⁴⁹ could also be synthesized.

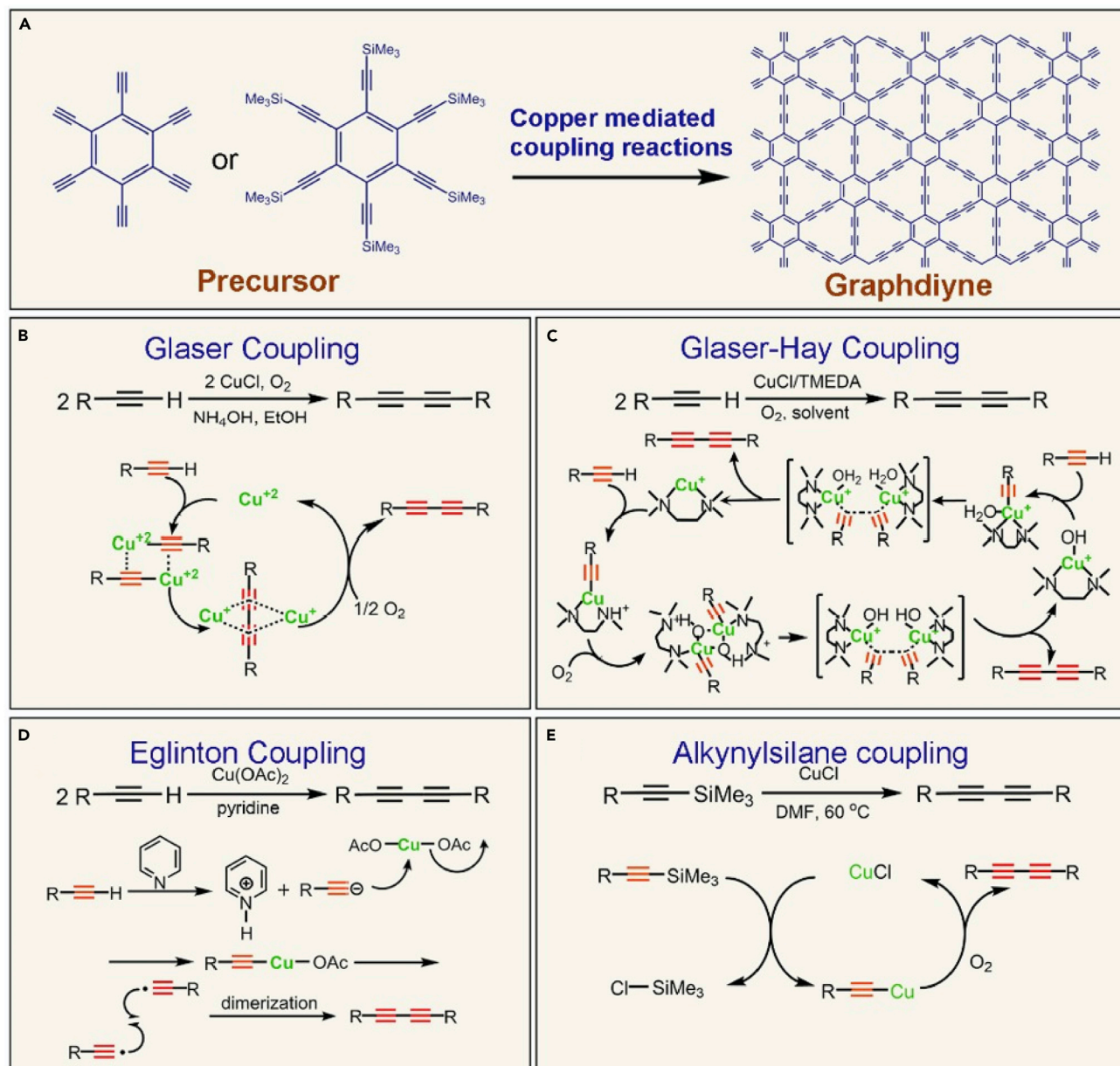


Figure 2. Synthetic Route and Cu-Mediated Acetylenic Coupling Reactions toward GDY

(A) Concluded synthetic route for GDY based on HEB or HEB-TMS precursor.

(B) Proposed mechanism for classical Glaser coupling reaction. Reprinted with permission from Zhou et al.³⁴ Copyright 2019 Wiley-VCH.

(C) Proposed mechanism for Glaser-Hay coupling reaction. Reprinted with permission from Sakamoto et al.⁴⁰ Copyright 2019 Wiley-VCH.

(D) Proposed mechanism for Eglinton coupling reaction. Reprinted with permission from Diederich et al.⁴⁴ Copyright 1992 by VCH Verlagsgesellschaft mbH, Germany.

(E) Proposed mechanism for alkynylsilane coupling reaction. Reprinted with permission from Li et al.³² Copyright 2011 American Chemical Society.

This Cu foil-assisted coupling reaction opened up a way for the emerging GDY nano-materials. However, a full understanding of the formation mechanism and explicit component characterizations are lacking.

Glaser-Hay Coupling Reaction

Based on the acetylenic coupling reactions, several curial evolutions on the controllable preparation of GDY have been made. For the first time, Liu's group reported a

Table 1. Reaction Conditions and Promising Application Fields of the Fundamental Acetylenic Coupling Reactions for GDY

Reactions	Precursor	Catalytic System	Temperature	Applications
Modified Glaser coupling	HEB	Cu, pyridine	60°C	field-emission; ³² energy storage; ⁵³ electroanalysis and electrochemistry ^{54,55}
Modified Glaser-Hay coupling	HEB	Cu, TMEAD, pyridine	50°C	field-emission; ²⁸ catalyst; ⁵² solar steam generation ⁵⁶ ; oil-water separation ⁵⁷
Eglinton coupling	HEB	Cu(OAc) ₂ , pyridine	Room temperature	gas sensor; ²¹ catalyst ⁵⁸
Alkynylsilane coupling	HEB-TMS	CuCl, DMF	65°C–70°C	field-effect transistor ²⁷

feasible synthetic route of GDY nanowalls via a modified Glaser-Hay coupling reaction,²⁸ whose reaction conditions were demonstrated in Table 1. The Glaser-Hay coupling was derived from the Glaser reaction and achieved an important improvement under the application of a catalytic amount of bidentate ligand N, N, N', N'-tetramethylethylenediamine (TMEDA).⁵⁰ The coupling reaction rate was considerably faster ascribed to the enhanced solubility of Cu-TMEDA complex, which experienced further oxidative coupling with O₂. According to the coupling mechanism based on DFT calculation proposed by Fomine et al., Cu(I)/Cu(III)/Cu(II)/Cu(I) catalytic cycle was involved for Glaser-Hay coupling and the dominant step was the dioxygen activation of Cu(I) complex for Cu(III) complex (Figure 2C).⁵¹ Glaser-Hay coupling reaction with a more active catalyst system could be applied in diverse organic solvents and lower temperatures. Therefore, the reaction temperature and time in the modified Glaser-Hay coupling reactions on the copper foil are relatively lower than those of modified Glaser coupling. Glaser-Hay-coupling-reaction-induced GDY nanowalls with highly conjugated electronic structure and uniform sharp character are considered to have excellent roles in the field-emission application area,²⁸ meanwhile their nanoporous networks and the abundant active sites are promising in the construction of high-performance catalysts.⁵²

Eglinton Coupling Reaction

According to the proposed mechanism of Glaser coupling and Glaser-Hay coupling, the existence of relevant base promotes the dehydrogenation of terminal alkyne and the production of acetylic copper intermediates. Afterward, these intermediates are dimerized in the presence of an oxidizing reagent such as O₂. In 1956, Eglinton and Galbraith introduced stoichiometric cupric salt catalyst in methanol-pyridine to promote the acetylenic coupling reaction.^{59,60} In the Eglinton coupling reaction, the dimerization could proceed in the absence of O₂ at room temperature. Klebansky et al. proposed that the reaction followed a radical mechanism with cupric ions as the oxidizing agents, and they also noted that the basic condition would enhance the reaction rate.⁶¹ Furthermore, Clifford et al. evolved this radical mechanism, showing that the Cu(I) acetylide species rapidly oxidized after the transfer of a single electron to Cu(II) through an acetate ligand bridge.⁶² As shown in Figure 2D, the decomposition of Cu(II) and recombination of the free alkynyl radicals resulted in coupled diyne products. Eglinton oxidative coupling reaction is well suited for the construction of macrocyclic acetylenes with diyne structure. Zhang and co-workers developed a facile strategy to confine the few-layered GDY on graphene substrate via Eglinton coupling using HEB and Cu(OAc)₂ as monomer and catalyst, respectively.²¹ The resulting GDY-graphene heterostructure films exhibited promising application as the gas sensor. Eglinton coupling reaction with a radical reaction mechanism endows the approach with mild conditions of low temperature and high efficiency.

This oxidative coupling reaction can be conducted smoothly in the interfaces of solution and substrate, and it can also be extended to other templates, such as h-BN, via π - π interactions. With mild reaction condition and excellent feasibility, Eglinton coupling reaction would pave the way for the design of diverse 2D acetylenic carbon allotropes.

Alkynylsilane Coupling Reaction

GDY can be considered as the molecular-based covalent organic nanosheet, despite that, they are all-carbon materials.⁴⁰ Hence, traditional synthetic strategies of GDY synthesis use terminal alkyne oxidative coupling reaction based on the designed HEB monomer. HEB molecules are conventionally produced from hexakis-(trimethylsilyl)ethynyl]benzene (HEB-TMS) after a deprotection reaction under inert atmosphere. Whereas, the HEB monomers with six alkynyl groups are not stable in the coupling reaction condition and would counter with oxidation and self-polymerization inevitably. Subtly, Liu and co-workers synthesized GDY on the graphene or h-BN template employing the HEB-TMS as the precursor, CuCl as the catalyst, and polar N,N-dimethylformamide (DMF) reagent as the solvent.²⁶ The GDY-based field-emission transistor demonstrated good conductivity and p-type characteristic. The corresponding reaction underwent Cu(I)-promoted homocoupling of alkynylsilane, referring to the observation by Hiyama et al. (Figure 2E).^{63,64} This alkynylsilane coupling reaction can smoothly proceed in the Cu(I) catalytic system in various polar solvents, such as DMF or dimethylsulfoxide (DMSO) with excellent yield (>99%). In the coupling reaction, alkynylsilanes turn into Cu(I)-acetylide intermediates, which further produce diynes in the presence of oxygen. Therefore, alkynylsilane coupling opens new horizons for the stable production of high-quality GDY.

As mentioned above, these Cu-mediated acetylenic coupling reactions have provided fundamental synthetic ideas for GDY. Glaser coupling catalyzed by Cu(I) was proposed first, and the other three coupling reactions that followed modified the catalyst systems. In the Glaser-Hay coupling reaction, the addition of bidentate ligand TMEDA could increase the reaction rate ascribed to improved solubility of Cu catalyst complex. In the Eglinton coupling reaction, cupric salt catalyst system under a radical mechanism endows it with high efficiency at room temperature. In the alkynylsilane coupling reaction, the utilization of alkynylsilane precursor could realize a much more stable reaction condition. Based on the catalytic mechanisms, improvements and modifications for the acetylenic coupling reactions can also be introduced for 1,3-diynes. CuAl-layered double hydroxide (LDH) catalyst where copper(II) is located has been investigated for acetylenic homocoupling reactions.⁶⁵ Low-cost Cu-LDH were discovered to be effective at room temperature in the coupling reactions in various substrates, exhibiting promising commercial applications. Harmful organic solvents in these acetylenic coupling reactions could be replaced with greener solvent alternatives, such as polyethyleneglycol,⁶⁶ ionic liquids,⁶⁷ supercritical CO₂,⁶⁸ and water.⁶⁹ Besides, electrochemical oxidation,⁷⁰ microwave irradiation,⁷¹ and ball milling⁷² have been found to be potential approaches to promote the coupling reactions for 1,3-diynes. These modifications and improvements of the catalytic systems in the coupling reactions could inspire the researcher to further search for new synthetic strategies of ideal GDY.

CONTROLLABLE SYNTHESIS OF GDY

Taking the above studies of coupling reactions into account, the wet chemical route is generally used through selecting reaction system for preparing GDY. It must also be mentioned that challenges still exist, leading to the uncontrollability of quality improvement of GDY, as shown in Figure 3. First, the stability of monomers is one of the most

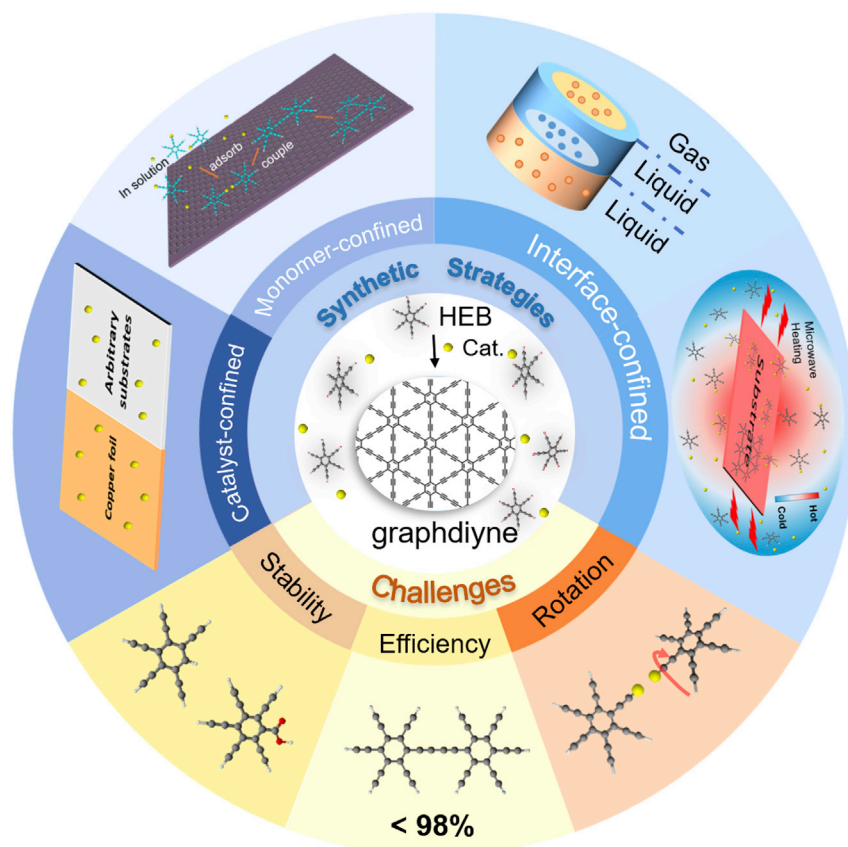


Figure 3. The Major Challenges and Strategies in Controllable Synthesis of GDY

Black ball and green ball, carbon atom; red ball, oxygen atom; white ball, hydrogen atom; yellow ball and blue ball, Cu catalyst; orange ball, HEB

important problems that need to be solved. The precursor (HEB) could easily turn brown without the protection of an inert gas because of the weak acidity and high reactivity of the terminal alkynyls.⁷³ In other words, HEB may form an acetylide-conjugated base, and the oxidative reactions will take place. Second, the low coupling efficiency with side reactions will introduce defects and influence the domain size of GDY structure.⁷⁴ Third, low rotation barrier existing at the alkyne-aryl single bonds lead to free rotation relative between the fragments.³⁴ These problems result in overlapping and unordered 3D GDY networks, which are far from the ideal GDY structure. Therefore, in order to obtain single- or few-layered GDY with a large domain size, some controllable synthetic strategies, namely catalyst, monomer, and interface-confined synthetic methods, are developed (Figure 3), which will be discussed in detail in this section. In traditional organic chemical synthetic methods, the reactants and catalysts are mixed in the solution and fully stirred to obtain the target products. However, intensive mixing of catalysts and monomers will increase the possibility of unordered coupling of monomers. In a confined synthetic method, the catalysts and monomers are respectively or simultaneously restricted near the target substrates by concentration diffusion, templet effect, interface, and temperature gradient, defining the places where the reaction occurs and solving the above problems.

Catalyst-Confined Synthetic Method

In catalyst-confined synthetic method, a concentration gradient of catalyst will form from substrate (high concentration) to solution (low concentration). The rate and

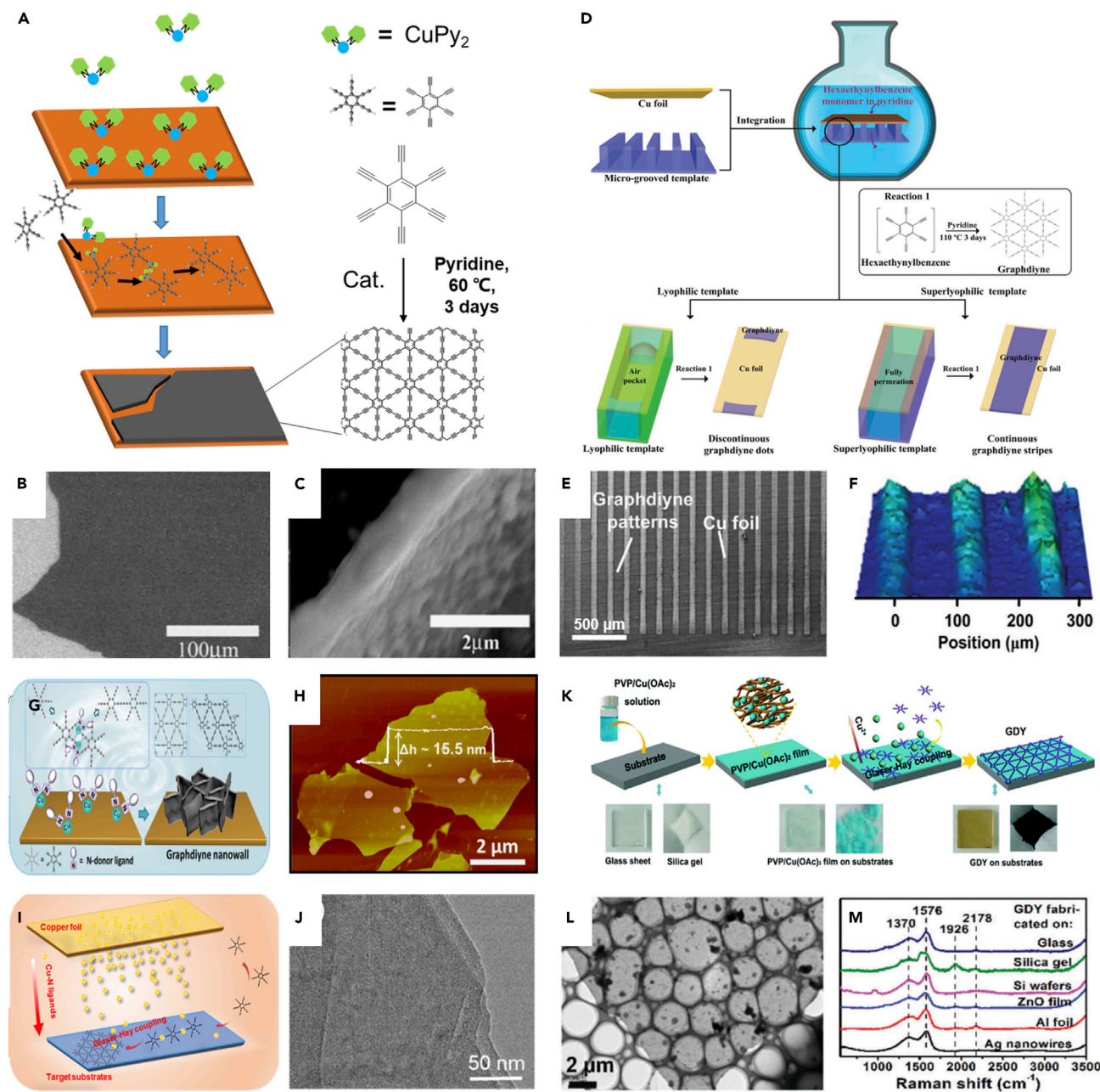


Figure 4. Catalyst-Confining Synthetic Method of GDY

(A–C) (A) Schematic illustration of coupling reaction on Cu surface. The SEM images of GDY films grown on the surface of copper foil, (B) large-area GDY film, and (C) a turned-up film. Reprinted with permission from Li et al.²⁴ Copyright 2010 The Royal Society of Chemistry.

(D–F) (D) Schematic illustration of the *in situ* synthesis of GDY linear patterns. The SEM image (E) and 3D Raman mapping (G-band) image (F) of GDY growth upon the copper foils. Reprinted with permission from Wang et al.⁴⁹ Copyright 2016 Wiley-VCH.

(G) Synthesis of GDY via *in situ* Glaser-Hay coupling reaction on Cu foils.

(H) AFM image of an exfoliated sample (G) on SiO₂/Si substrate. Reprinted with permission from Zhou et al.²⁸ Copyright 2015 American Chemical Society.

(I) Synthesis of GDY nanowalls on arbitrary substrates via copper envelope catalysis.

(J) HRTEM images of GDY nanowalls. Reprinted with permission from Gao et al.²⁹ Copyright 2016 WILEY-VCH.

Figure 4. Continued

(K) Schematic illustration of the fabrication of GDY on arbitrary substrates with the controlled release method and the photos of the fabricating process on the glass substrate and silica gel.

(L) TEM images of as-prepared GDY on Al foil.

(M) Typical Raman spectra of GDY fabricated on different substrates. Reprinted with permission from Zhao et al.⁷⁵ Copyright 2018 The Royal Society of Chemistry.

efficiency of the alkyne-coupling reaction increase because of the sufficient catalysts near the surface of target substrate. Employing catalyst-confined synthetic method, GDY films, stripe arrays, and nanowalls can be obtained not only on the copper foils but also on the arbitrary substrates. Li and co-authors first generated GDY nanoscale films with 1- μm thickness on the surface of the copper foil, which served as the substrate and source of catalyst using Glaser coupling reaction in 3 days (Figure 4A).²⁴ Cu(II) catalysts turn out forming a concentration gradient from copper foils to solution in the presence of pyridine without stirring. Near the copper foils, the concentration of catalysts is higher and the monomer (HEB) coupling reaction is faster than that in the solution. As a result, GDY films with large areas can be synthesized on the copper foils.

Through association of a template technique, Jiang and co-workers prepared the GDY stripe arrays.⁴⁹ In the reaction solution with HEB and pyridine, a superlyophilic grooved template forms a close contact with a flat copper producing numerous of microscale reaction channels (Figure 4D) to restrict the space of the reaction process. Since the Cu-pyridine catalyst was formed and diffused into the linear channels, the HEB cross-coupling reaction happened and the ordered GDY stripes would appear upon the copper-pillar-gap regions as shown in the scanning electron microscopy (SEM) image (Figure 4E). The G-band Raman mapping image of the GDY stripes on a silicon wafer (Figure 4F) shows regular green stripes and consists with the SEM observation of the GDY stripes.

To improve the efficiency of alkyne coupling, a modified Glaser-Hay coupling was employed to synthesize GDY nanowalls on copper foils, as shown in Figure 4G.²⁸ Atomic force microscopy (AFM) image (Figure 4H) of an exfoliated GDY nanowall on a SiO_2 -Si plate indicated the layered structure with a thickness of about 15 nm. TMEDA was introduced as a stronger N-ligand with a rapid reaction rate and higher efficiency for the alkyne coupling reaction in acetone compared with that in pyridine. On the other hand, HEB is more stable in acetone than in pyridine, due to the weak acidity of acetone. For the purpose of avoiding the limitations associated with substrates, an envelope method was developed to fabricate GDY nanowalls on arbitrary substrates,²⁹ including 1D (Si nanowires), 2D (Au, Ni, W foils, and quartz), and even 3D substrates (stainless steel mesh and graphene foam [GF]), which expanded the range of applications. In this strategy, target substrates were tightly wrapped by copper foils, and Cu ions acted as the "running catalysts" generated from copper foils and arrived at the surface of target substrates where the monomers react (Figure 4I).

Huang and co-workers reported an *in situ* growth of GDY on arbitrary substrates through a catalyst-controlled release method using Eglinton coupling reaction.⁷⁵ As the description of Figure 4K, polyvinylpyrrolidone/copper(II)-acetate (PVP/ $\text{Cu}(\text{OAc})_2$) films were formed on the target substrates. Cu(II) ions were released into the solution and formed a concentration gradient from substrate to bulk solution. The thickness of the GDY films can be regulated by altering the amounts of $\text{Cu}(\text{OAc})_2$ in PVP/ $\text{Cu}(\text{OAc})_2$ composite films. However, the macroscopic GDY films are aggregated with different angles of GDY sheets; thus, the differences in the

reaction environment, including the surface morphology of substrates and release rates of catalysts, will influence the GDY aggregations.⁷⁵

Although GDY nanowalls, stripe arrays, and films have been successfully fabricated via catalyst-confined synthetic method, the ultrathin GDY films are still difficult to be prepared using this strategy, since the formed copper ions diffuse from substrate to bulk solution, resulting in a weak catalyst concentration gradient from substrate to bulk solution. Thus, the catalyst-confined synthetic method should improve in decreasing the range of catalyst. It might be a good idea to introduce an external field, such as electric field and magnetic field, to control the move direction and confine the catalyst to facilitate the adsorption on substrate surface. Then the coupling reaction will be confined in a limited space to obtain single- or few-layered GDY.

Monomer-Confined Synthetic Method

The uncontrollable thickness, lability of HEB, and free rotation of carbon-carbon single bond between diacetylene are barriers for successful preparation of single- or few-layered GDY. In order to solve these problems, a valid synthetic method was developed to synthesize trilayer crystal GDY stacked on graphene (Figure 5A) through a van der Waals (vdW) epitaxial strategy.²¹ Graphene is an ideal candidate used as the epitaxial substrate to synthesize 2D materials, such as 2D covalent organic framework (COF) films⁷⁶ and strained pentacene thin films.⁷⁷ Benefiting with π - π and vdW interaction between HEB and graphene, HEBs favor coupling with each other in plane rather than out of plane to prevent the free rotation between fragments. The controllable experiment indicated GDY only grow on graphene rather than SiO₂/Si substrate. First-principles calculations showed that the HEB molecules were absorbed to the surface of graphene with flat-lying geometry and binding energy of 1.47 eV. Energy barriers of the rate-determining step as well as reaction energies are lower than those in solution, which facilitates the growth of few-layered GDY films. It is worth noting that aberration-corrected high-resolution transmission electron microscopy (HRTEM) imaging (Figure 5B) observed on GDY-graphene heterostructure films domain implied an ordered 2D GDY structure, and the typical Raman spectra randomly collected of GDY on graphene (Figure 5C) verified the continuity of GDY at the macroscopic scale. The vdW epitaxial substrate was also expanded to the hexagonal boron nitride (hBN), which has similar structure with graphene. The expansion was beneficial for fine characterization of intrinsic properties of GDY and possesses potential applications in the field of photoelectric devices.

To further avoid the oxidation of monomer, Liu and co-workers also adopted HEB-TMS molecules as precursors and used alkynylsilane coupling reaction to fabricate GDY films on graphene templet (Figure 5D).²⁶ Through the epitaxial growth strategy, a continuous flat ultrathin GDY film with a thickness of about 3–4 nm was synthesized successfully. Moreover, taking advantages of graphene-templated method, ultrathin β -GDY-like films could be synthesized using tetraethynylethene (TEE) as the precursor by Eglinton coupling reaction (Figure 5G).²⁷ The thickness of β -GDY-like films containing single-layered graphene characterized by AFM is about 1.5 nm. HRTEM image (Figure 5H) showed uniform lattice fringes, which reflected the ordered structure of the films. The typical Raman spectra (Figure 5I) of the β -GDY-like films on graphene at different positions was consistent with theoretical predictions. Electrical measurement revealed that the films presented a conductivity of $1.30 \times 10^{-2} \text{ S} \cdot \text{m}^{-1}$, which presented a great improvement compared with previous work.⁷⁸

Monomer-confined synthetic method benefits from the vdW and π - π interactions between HEB and substrates (graphene and h-BN) to solve the problems of uncontrollable thickness, the lability of monomers, and the free rotation of carbon-carbon

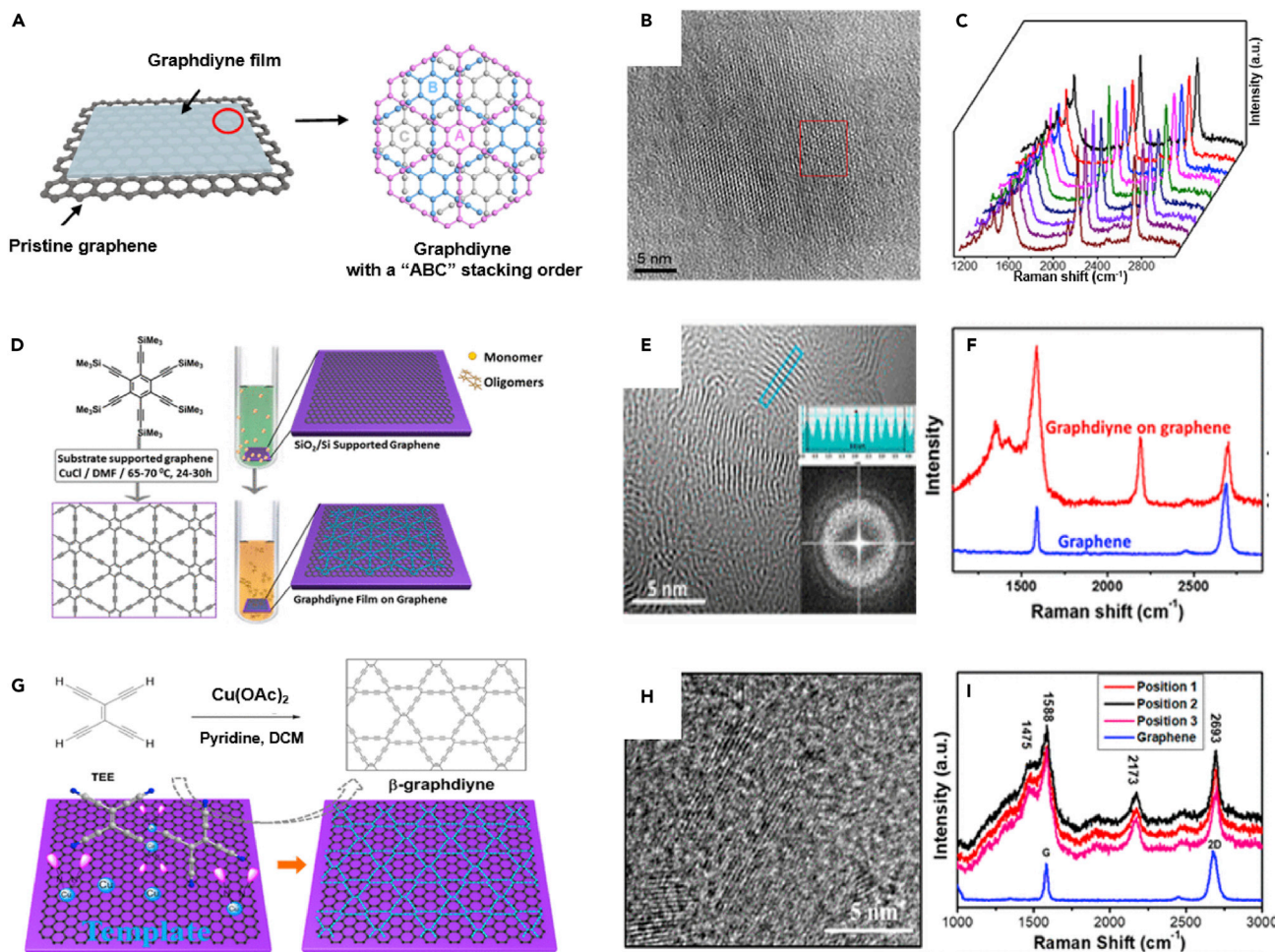


Figure 5. Monomer-Confined Synthetic Method

(A) Synthesis of GDY via Eglinton coupling reaction.

(B) Aberration-corrected HRTEM imaging of GDY domain.

(C) Typical Raman spectra randomly collected of GDY on graphene. Reprinted with permission from Gao et al.²¹ Copyright 2018 American Association for the Advancement of Science.

(D) Synthesis of GDY via alkyne-silane coupling.

(E) HRTEM image of transferred GDY films.

(F) Raman spectra evolution of graphene and as-grown GDY on graphene. Reprinted with permission from Zhou et al.²⁶ Copyright 2018 American Chemical Society.

(G) Synthesis of β -GDY-like films on graphene via Eglinton coupling.

(H and I) HRTEM image (H) and Raman spectra (I) of the β -GDY-like films on graphene. Reprinted with permission from Li et al.²⁷ Copyright 2019 American Chemical Society.

single bond between the diacetylenic linkages. However, the strong interaction between GDY and graphene makes it difficult to separate independent GDY films, which limits the studies of intrinsic properties and applications. Thus, it is better to select an appropriate epitaxial templet and combine with feasible approaches, which avail the growth of single- or few-layer GDY and easy separation of GDY from substrates.

Interface-Confined Synthetic Method

Growing 2D polymeric materials at solid-liquid,^{79,80} liquid-liquid,^{81–83} or gas-liquid^{84–86} interfaces, such as surface COFs and surface metal-organic frameworks

(MOFs), are already widely used methods. There are three main advantages of using the interfaces for GDY preparation: (1) the flat and uniform interface space on a large length scale; (2) the availability of the liquid subphase as a pool of monomers and catalysts; and (3) the straightforward preparation and transfer without damage onto target substrates.⁸⁶ In this section, considering the challenges of solution method, interface-confined synthetic method is proposed to synthesize few-layered GDY films through restricting the reaction taking place in a limited space. Nishihara and co-workers reported a liquid-liquid and gas-liquid interfacial synthesis of GDY.²² First, they used dichloromethane-containing HEB monomer and catalysts (copper(II) acetate and pyridine) aqueous that are nearly immiscible (Figure 6A). GDY films were gradually generated on the interface of two solutions in the presence of HEB and catalyst at room temperature (Figure 6B). The GDY films have a sheet morphology with lateral dimensions of 25–100 μm and a thickness of 24 nm. TEM (Figure 6C) and selected area electron diffraction (SAED) revealed the good crystallinity of the GDY films. The gas-liquid interfacial synthetic route is shown in Figure 6E. A mixture organic solvent with a lower concentration of monomers was gently added dropwise to the surface of the catalysts aqueous under an inert argon protection. When the organic solvent quickly volatilizes, the coupling reaction take place at the gas-water interface, and GDY nanosheets will float on the interface. Then a number of regular hexagonal shape nanosheets with 1–2 μm diagonal length could be observed by TEM (Figure 6F), which accords with the hexagonal crystal lattice of GDY. AFM analysis showed a thickness of ~ 3.0 nm and smooth hexagonal domains on HMDS/Si (100). The Raman spectra (Figure 6G) showed the typical C-C bonding of GDY. To prepare large-area GDY ultrathin films, Hu and co-workers modified the gas-liquid interface-confined synthetic method in an air atmosphere⁸⁷ as described in Figure 6H. The centimeter-scale and freestanding GDY ultrathin films were obtained by this method and can be easily transferred to arbitrary solid substrates, which is suitable for device fabrication.

To further take advantage of the interface, Zhang and co-authors developed a rapid temperature gradient solid-liquid interface synthetic strategy. Microwave irradiation was introduced to produce the temperature gradient and promoted the process of coupling reactions without catalyst (Figure 6K).²³ The sodium chloride (NaCl) was selected as the substrate that can adsorb microwave and a mixture of toluene and hexane (1:1 v:v) served as a non-adsorbing solvent. After microwave irradiation of 4 min (700 W), the temperature of NaCl increased to about 70°C, which is favorable for monomer coupling reactions. On the contrary, the monomers in the solvent were more stable and could diffuse to the surface of the substrates. Unlike the traditional Glaser coupling reaction, microwave can assist the homolytic cleavage of C-H bond to form an acetylenic radical and couple to fabricate GDY films with an average thickness of less than 2 nm in the absence of the catalysts. Raman spectrum (Figure 6M) of as-synthesized films confirmed the successful coupling of alkyne group. HRTEM image (Figure 6L) of GDY films evidenced the high crystallinity.

It is valid that constructing the interface of gas-liquid and liquid-liquid limit the coupling reaction space to obtain GDY nanosheets and films. The thickness of GDY is difficult to control because of the interdiffusion layer between water and organic solvent. The air-water interface goes against the stability of monomers leading to defects and amorphous structure. Notably, the introduction of temperature gradient in association with microwave heating is an efficient method. Not only the stability of the HEB is guaranteed but also the high efficiency of the coupling reaction assisted with microwave can enhance the formation of ordered GDY structure.

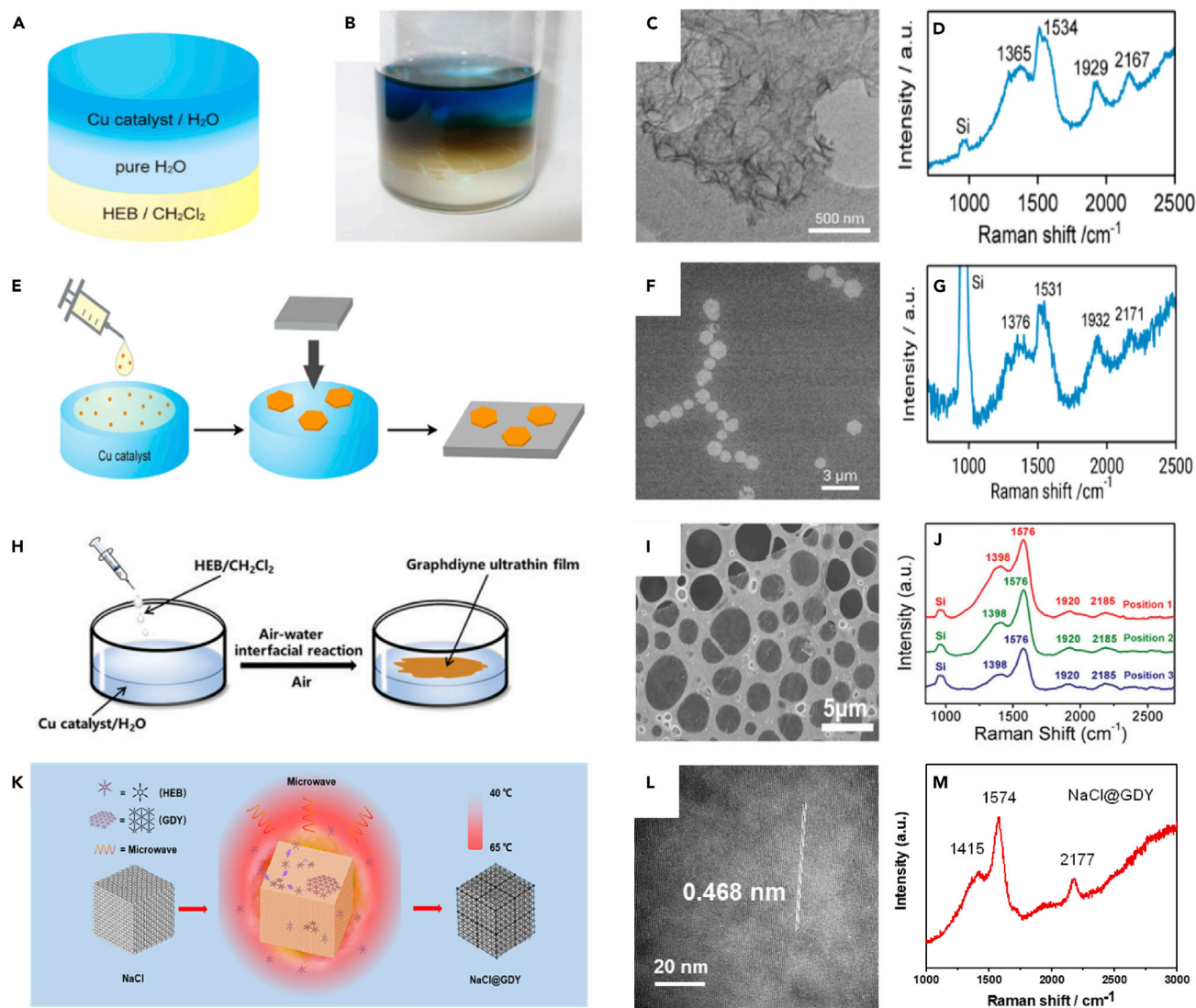


Figure 6. Interface-Confined Synthetic Method

(A and B) Schematic illustration (A) and a photograph (B) of the GDY liquid-liquid interfacial synthetic procedure.

(C and D) TEM image (C) and Raman spectrum (D) of multilayer GDY.

(E) Schematic illustration of the gas-liquid interfacial synthesis and transfer process.

(F and G) TEM micrograph on an elastic carbon grid (F) and Raman spectrum (G) of hexagonal GDY nanosheets. Reprinted with permission from Matsuoka et al.²² Copyright 2016 American Chemical Society.

(H) Schematic illustration of the synthetic process of GDY thin films at the air/water interface.

(I) SEM image of the GDY film on a holey carbon matrix.

(J) Raman spectra of the GDY film on three arbitrary positions. Reprinted with permission from Li et al.⁸⁷ Copyright 2020 The Royal Society of Chemistry and the Chinese Chemical Society.

(K) Schematic presentation of the microwave-assisted synthesis process of GDY films.

(L and M) HRTEM images (L) and Raman spectrum (M) of GDY films. Reprinted with permission from Yin et al.²³ Copyright 2020 Wiley-VCH.

The drawback of microwave heating NaCl substrate is small-area GDY films because of the small size of substrate. Thus, adopting other heat sources, such as radio frequency (RF) heating, to expand GDY growth substrates may be the future direction. As we all know, eddy currents will be generated within the metal under the RF induction. Thus, continuous large-area GDY films may be synthesized on metal foils, including Cu, Ag, and Au substrate, where temperature gradient form with the aid of RF heating.

SCALE-UP PRODUCTION OF GDY

Although relatively high-crystalline and few-layer GDY are synthesized in the liquid and gas phases via some controllable synthetic methods, it is very industrially valuable to find a simple synthetic strategy to synthesize GDY in large scale. In the past few years, several *in situ* methods have been developed for massive production of GDY, leading to advanced applications. Li and co-workers reported an *in situ* Glaser coupling process to synthesize Cu@GDY core-shell nanowires array for high-efficient hydrogen evolution cathode in 2016.⁸⁸ In 2017, they reported *in situ* Eglinton coupling process to synthesize ultrathin GDY nanosheets on copper nanowires as lithium-ion battery anodes.³¹ Lu and co-workers developed an *in situ* Glaser-Hay coupling method to synthesize CdS-GDY heterojunction for enhanced photocatalytic activity of hydrogen production in 2018.⁸⁹ Almost all the reported methods require metallic copper as a substrate, which severely limits the yield of GDY and its large-scale application because of the high cost and low specific surface area (SSA) of copper substrate. Most efforts were devoted to the synthesis of GDY compounds with other substances and gained great performance improvement in various fields. However, large-scale synthesis of monocrystalline GDY still remains a burning question and needs to be solved urgently.

Explosion Method

In 2017, Li and co-workers reported an explosion method to synthesize large-scale GDY powder in a very short time for an advanced battery anode application.⁹⁰ In this method, HEB could homogeneously couple with each other in the solid phase, which means almost every HEB could react to prepare GDY, leading to the high yield of GDY (up to 98%). GDY powders with three different morphologies, including GDY nanoribbons, 3D GDY framework, and GDY nanochains, were synthesized by simply changing the atmosphere and heating rate of HEB precursors.

3D Substrates-Mediated Synthesis of GDY

Although a large scale of GDY powders can be gained rapidly with the explosion method, some problems are still unsolved, including monomer stability, side reactions, and orientation. On a proper substrate, HEB molecule can be forced into one plane when coupling reactions occur. Obviously, the yield of GDY depends on the surface area of substrate. In order to increase the yield of GDY, hierarchical GDY-based architecture is synthesized for efficient solar steam generation using copper foam-coated CuO coaxial nanowires as substrate that has higher surface area than copper foil (Figure 7A).⁵⁶ Figures 7B and 7C show the well-controlled structures of GDY coated on CuO nanowires. The quality of GDY could be further evidenced by the Raman spectrum shown in Figure 7D, where the peak at $2,178.9\text{ cm}^{-1}$ can be assigned to the vibration of conjugated diyne links, indicating highly ordered GDY were successfully prepared.

However, the yield of GDY is still restricted by the low production and high cost of 3D copper foam. The weight of the GDY-based architecture was mainly from the substrate. The surface area of substrate was not large enough to support GDY. The control and regulation of such copper-substrate-based method have become more and more delicate, and more ingenious design is needed to synthesize large-scale GDY with high crystalline. To further increase the yield of GDY, a naturally abundant diatomite was used as a template to prepare freestanding 3DGDY powder (Figure 7E).³³ Diatomite has a hierarchical porous structure and large surface area, providing a feasible way for massive production of GDY with low cost, which would really give opportunity to future industrial preparation and application. In this method, copper nanoparticles (CuNPs) were primarily absorbed on the surface and in the holes of

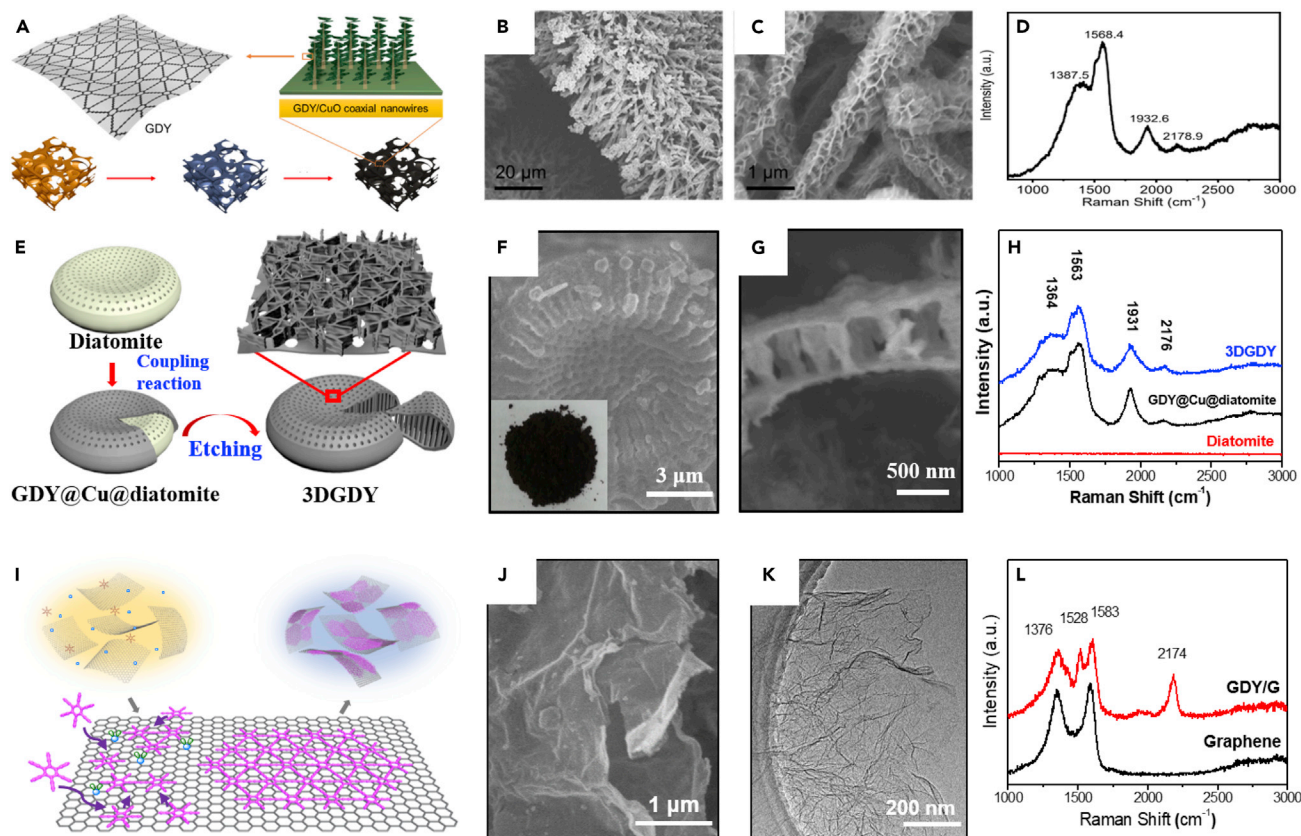


Figure 7. Scale-Up Production of GDY

(A) Schematic illustration of GDY-based hierarchical architecture.

(B and C) SEM images of the copper foam coated by GDY-CuO coaxial nanowires.

(D) Typical Raman spectrum of GDY nanowalls grown on nanowires. Reprinted with permission from Gao et al.⁵⁶ Copyright 2017 American Chemical Society.

(E) Schematic illustration of the experimental setup for the 3DGDY synthesis using diatomite as template.

(F and G) SEM images of 3DGDY.

(H) Raman spectra of 3DGDY, GDY@Cu@diatomite, and diatomite. Reprinted with permission from Li et al.³³ Copyright 2018 Wiley-VCH.

(I) Schematic illustration of the experimental setup for the GDY/G heterostructure synthesis through a solution-based vdW epitaxy method.

(J and K) SEM (J) and (K) TEM images of GDY/G.

(L) Raman spectra GDY/G and reduced graphene oxide (rGO). Reprinted with permission from Li et al.⁵⁸ Copyright 2019 Wiley-VCH.

diatomite. Then the alkyne coupling reaction occurred on the diatomite surface. After the reaction completed, diatomite was wrapped in GDY flakes (GDY@Cu@diatomite). Porous 3DGDY with freestanding structure was obtained after carefully removing the residual copper and diatomite by etching reagents. Figure 7F shows the round cake-like 3DGDY after etching diatomite and CuNPs. Figure 7G displays the internal structure of 3DGDY, in which the GDY flakes are connected by hollow GDY columns that play the key role in protecting the freestanding structure of 3DGDY from collapsing. Figure 7H shows typical Raman spectra of 3DGDY, GDY@Cu@diatomite, and diatomite, in which four dominant peaks appear at 1,364, 1,563, 1,931, and 2,176 cm^{-1} in Raman spectrum of 3DGDY. Two bands at 1,931 and 2,176 cm^{-1} are derived from the vibration of the conjugated diyne linkage and carbon-carbon triple bond, respectively, which reveal the highly ordered GDY powders.

Massive Production of GDY/Graphene Heterostructure

Based on the above discussion, there are two main strategies to achieve large-scale production of GDY: direct synthesis of GDY in solid phase and on a substrate with

large surface area. Although direct synthesis in solid phase with explosion method could gain a high yield of GDY up to 98%, most area of GDY still remain amorphous, which may result from the large energy burst in a short time, making HEB unstable and with no substrate or interface, the HEB molecule could rotate during the reaction. With the increasing surface area of the substrate, the yield of GDY could increase. The traditional solid substrate with high surface area could not have a strong enough interaction with GDY or HEB, which means HEB may rotate during reaction, and the quality of GDY will still have room for improvement. Considering the facile synthesis of an ultrathin single-crystalline GDY film on graphene through a solution-phase vdW epitaxial strategy,²¹ the liquid-exfoliated graphene with large-scale production, low cost, and high surface area was used as an epitaxy template to achieve massive production of few-layered GDY with high crystallinity (Figure 7I).⁵⁸ Graphene sheets were prepared from graphite through liquid exfoliation and were dispersed in pyridine. Then, Eglinton coupling reaction was carried out in the presence of HEB and Cu(OAc)₂ at room temperature. Thanks to the vdW interaction and lattice match between GDY and graphene, few-layered GDY grew on both sides of the graphene sheets. The SEM image of GDY/graphene (GDY/G) is shown in Figure 7J, in which GDY/G heterostructure maintains the morphology of graphene with increased thickness. TEM image in Figure 7K confirmed that the morphology of GDY/G was consistent with that of graphene sheets, indicating the in-plane growth of GDY on graphene. Figure 7L showed the typical Raman spectra of different samples. Distinct peak at 2,174 cm⁻¹ could be clearly seen in the Raman spectra of GDY/G, indicating highly ordered GDY.

By controlling the surface area of the substrate, utilizing the solid/liquid interface, and employing graphene as a surface template, the yield and quality of GDY were well improved. Up to now, the SSA of GDY/G powder was measured to be as high as 390.6 m²·g⁻¹, which was more than 3-fold higher than that of pristine GDY powder. The achievement in GDY powder synthesis would contribute a lot to the applications and research in various domains. Based on the above discussion, the bottom-up methods to synthesize large-scale highly ordered GDY have the following key points: (1) the surface area of substrate determines the yield of GDY and (2) the presence and the templating effect of substrate determine the quality of GDY. It is possible to precisely control the amount of GDY powder and the quality. Moreover, doped GDY or other types of GDY with unique properties can also be obtained by the methods discussed above. We can see that great progress will be made for yield and quality improvement.

CONCLUSIONS

GDY has attracted great concern since it was first proposed, and much efforts have been devoted to exploring the synthetic methods of single or few-layered GDY since the theoretical 2D features of GDY and its unprecedented chemical and physical properties. However, a gap still exists between the ideality and reality of GDY due to the existence of real problems and challenges during synthetic processes of GDY that lead to difficulties to obtain single- or few-layered GDY with large-area and long-ordered structure. This review summarizes the latest progress on synthetic methodology of GDY in the aspect of basic acetylenic coupling reactions, controllable synthetic methods, and scale-up production. Cu-mediated wet chemical synthetic processes have been demonstrated to be ideal methods to synthesize GDY. The thickness and crystallinity of GDY can be well controlled through the developed confined methods taking advantage of catalyst concentration gradient, vdW epitaxy, interfacial space, and temperature gradient, such as catalyst, monomer,

and interface-confined synthetic methods. In addition, accessible methods show fine-tuned growth of few-layered GDY with large crystal domain. In order to approach the practical applications, some massive production methods are developed to synthesize large-scale GDY via controlling the surface area of substrate, even employing an epitaxy substrate with high surface area. As a result, powder-like GDY/G heterostructure with the surface area as high as $390.6 \text{ m}^2 \cdot \text{g}^{-1}$ was prepared with high crystallinity and yield, which provides a great possibility for the industrial applications of GDY in the future.

These typical works shown above offer the unprecedented opportunities in crystallinity and structural robustness. Especially developing a feasible method to obtain the monolayered single crystal GDY is vital. However, this would not be an easy case and several challenges have to be resolved. For instance, investigating appropriate reaction conditions to improve the stability of monomers and coupling efficiency form the foundation. At the same time, confined growth also can be evolved through introducing external field (e.g., photosource, electrostatic field, magneto-static field, and dynamic electromagnetic field at different frequencies). It is crucial to develop a common approach of mass production for practical applications. On the other side, GDY, a novel 2D carbon materials, should find killer applications on the basis of intrinsic properties. GDY has a uniformly distributed porous framework, large π -conjugated systems, and appropriate band gap exerting promising potential in the separation of mixed gases, water remediation, catalysis, and energy-related fields. We believe that the gap will be bridged through rational design and synthetic methods in the future.

ACKNOWLEDGMENTS

This research was supported by the Ministry of Science and Technology of China (2016YFA0200104 and 2018YFA0703502) and the National Natural Science Foundation of China (51720105003, 21790052, 21974004).

AUTHOR CONTRIBUTIONS

J.Z., L.T., and J.L. proposed the topic of the review. Y.K., J.L., S.Z., and C.Y. investigated the literature and wrote the manuscript. Y.K. and J.L. contributed equally to this work. J.L., L.T., and J.Z. discussed and revised the manuscript.

REFERENCES

1. Zhang, H., Xia, Y., Bu, H., Wang, X., Zhang, M., Luo, Y., and Zhao, M. (2013). Graphdiyne: A promising anode material for lithium ion batteries with high capacity and rate capability. *J. Appl. Phys.* **113**, 044309.
2. Tang, H., Hessel, C.M., Wang, J., Yang, N., Yu, R., Zhao, H., and Wang, D. (2014). Two-dimensional carbon leading to new photoconversion processes. *Chem. Soc. Rev.* **43**, 4281–4299.
3. Srinivasu, K., and Ghosh, S.K. (2012). Graphyne and graphdiyne: promising materials for nanoelectronics and energy storage applications. *J. Phys. Chem. C* **116**, 5951–5956.
4. Zuo, Z., and Li, Y. (2019). Emerging electrochemical energy applications of graphdiyne. *Joule* **3**, 899–903.
5. Wu, P., Du, P., Zhang, H., and Cai, C. (2014). Graphdiyne as a metal-free catalyst for low-temperature CO oxidation. *Phys. Chem. Chem. Phys.* **16**, 5640–5648.
6. Huang, C., Li, Y., Wang, N., Xue, Y., Zuo, Z., Liu, H., and Li, Y. (2018). Progress in research into 2D Graphdiyne-based materials. *Chem. Rev.* **118**, 7744–7803.
7. Ren, H., Shao, H., Zhang, L., Guo, D., Jin, Q., Yu, R., Wang, L., Li, Y., Wang, Y., Zhao, H., and Wang, D. (2015). A new graphdiyne nanosheet/Pt nanoparticle-based counter electrode material with enhanced catalytic activity for dye-sensitized solar cells. *Adv. Energy Mater.* **5**, 1500296.
8. Qi, H., Yu, P., Wang, Y., Han, G., Liu, H., Yi, Y., Li, Y., and Mao, L. (2015). Graphdiyne oxides as excellent substrate for electroless deposition of Pd clusters with high catalytic activity. *J. Am. Chem. Soc.* **137**, 5260–5263.
9. Hui, L., Xue, Y., Yu, H., Liu, Y., Fang, Y., Xing, C., Huang, B., and Li, Y. (2019). Highly efficient and selective generation of ammonia and hydrogen on a Graphdiyne-based catalyst. *J. Am. Chem. Soc.* **141**, 10677–10683.
10. Jiao, Y., Du, A., Hankel, M., Zhu, Z., Rudolph, V., and Smith, S.C. (2011). Graphdiyne: a versatile nanomaterial for electronics and hydrogen purification. *Chem. Commun. (Camb.)* **47**, 11843–11845.
11. Cranford, S.W., and Buehler, M.J. (2012). Selective hydrogen purification through graphdiyne under ambient temperature and pressure. *Nanoscale* **4**, 4587–4593.
12. Liu, J., Chen, C., and Zhao, Y. (2019). Progress and prospects of Graphdiyne-based materials in biomedical applications. *Adv. Mater.* **31**, e1804386.
13. Long, M., Tang, L., Wang, D., Li, Y., and Shuai, Z. (2011). Electronic structure and carrier mobility in graphdiyne sheet and nanoribbons: theoretical predictions. *ACS Nano* **5**, 2593–2600.
14. Narita, N., Nagai, S., Suzuki, S., and Nakao, K. (1998). Optimized geometries and electronic

- structures of graphyne and its family. *Phys. Rev. B* **58**, 11009–11014.
15. Bu, H., Zhao, M., Wang, A., and Wang, X. (2013). First-principles prediction of the transition from graphdiyne to a superlattice of carbon nanotubes and graphene nanoribbons. *Carbon* **65**, 341–348.
 16. He, J., Ma, S.Y., Zhou, P., Zhang, C.X., He, C., and Sun, L.Z. (2012). Magnetic properties of single transition-metal atom absorbed graphdiyne and graphyne sheet from DFT+U calculations. *J. Phys. Chem. C* **116**, 26313–26321.
 17. Luo, G., Qian, X., Liu, H., Qin, R., Zhou, J., Li, L., Gao, Z., Wang, E., Mei, W.N., Lu, J., et al. (2011). Quasiparticle energies and excitonic effects of the two-dimensional carbon allotrope graphdiyne: theory and experiment. *Phys. Rev. B* **84**, 075439.
 18. Zheng, Q., Luo, G., Liu, Q., Quhe, R., Zheng, J., Tang, K., Gao, Z., Nagase, S., and Lu, J. (2012). Structural and electronic properties of bilayer and trilayer graphdiyne. *Nanoscale* **4**, 3990–3996.
 19. Guo, J., Shi, R.C., Wang, R., Wang, Y.Z., Zhang, F., Wang, C., Chen, H.L., Ma, C.Y., Wang, Z.H., Ge, Y.Q., et al. (2020). Graphdiyne-polymer nanocomposite as a broadband and robust saturable absorber for ultrafast photonics. *Laser Photonics Rev.* **14**, 1900367.
 20. Haley, M.M., Barand, S.C., and Pak, J.J. (1997). Carbon networks based on dehydrobenzoannulenes. 4. Synthesis of "star" and "trefoil" graphdiyne substructures via sixfold cross-coupling of hexaiodobenzene. *Angew. Chem. Int. Ed. Engl.* **36**, 3893–3901.
 21. Gao, X., Zhu, Y., Yi, D., Zhou, J., Zhang, S., Yin, C., Ding, F., Zhang, S., Yi, X., Wang, J., et al. (2018). Ultrathin graphdiyne film on graphene through solution-phase van der Waals epitaxy. *Sci. Adv.* **4**, eaat6378.
 22. Matsuoka, R., Sakamoto, R., Hoshiko, K., Sasaki, S., Masunaga, H., Nagashio, K., and Nishihara, H. (2017). Crystalline graphdiyne nanosheets produced at a gas/liquid or liquid/liquid interface. *J. Am. Chem. Soc.* **139**, 3145–3152.
 23. Yin, C., Li, J.Q., Li, T.R., Yu, Y., Kong, Y., Gao, P., Peng, H.L., Tong, L.M., and Zhang, J. (2020). Catalyst-free synthesis of few-layer graphdiyne using a microwave-induced temperature gradient at a solid/liquid interface. *Adv. Funct. Mater.* **30**, <https://doi.org/10.1002/adfm.202001396>.
 24. Li, G., Li, Y., Liu, H., Guo, Y., Li, Y., and Zhu, D. (2010). Architecture of graphdiyne nanoscale films. *Chem. Commun. (Camb.)* **46**, 3256–3258.
 25. Yan, H., Yu, P., Han, G., Zhang, Q., Gu, L., Yi, Y., Liu, H., Li, Y., and Mao, L. (2019). High-yield and damage-free exfoliation of layered graphdiyne in aqueous phase. *Angew. Chem. Int. Ed. Engl.* **58**, 746–750.
 26. Zhou, J.Y., Xie, Z.Q., Liu, R., Gao, X., Li, J.Q., Xiong, Y., Tong, L.M., Zhang, J., and Liu, Z.F. (2019). Synthesis of ultrathin graphdiyne film using a surface template. *ACS Appl. Mater. Interfaces* **11**, 2632–2637.
 27. Li, J., Xiong, Y., Xie, Z., Gao, X., Zhou, J., Yin, C., Tong, L., Chen, C., Liu, Z., and Zhang, J. (2019). Template synthesis of an ultrathin beta-graphdiyne-like film using the eglinton coupling reaction. *ACS Appl. Mater. Interfaces* **11**, 2734–2739.
 28. Zhou, J., Gao, X., Liu, R., Xie, Z., Yang, J., Zhang, S., Zhang, G., Liu, H., Li, Y., Zhang, J., et al. (2015). Synthesis of graphdiyne nanowalls using acetylenic coupling reaction. *J. Am. Chem. Soc.* **137**, 7596–7599.
 29. Gao, X., Li, J., Du, R., Zhou, J., Huang, M.Y., Liu, R., Li, J., Xie, Z., Wu, L.Z., Liu, Z., and Zhang, J. (2017). Direct synthesis of graphdiyne nanowalls on arbitrary substrates and its application for photoelectrochemical water splitting cell. *Adv. Mater.* **29**, 1605308.
 30. Jia, Z.Y., Li, Y.J., Zuo, Z.C., Liu, H.B., Li, D., and Li, Y.L. (2017). Fabrication and electroproperties of nanoribbons: carbon ene-Yne. *Adv. Electron. Mater.* **3**, 1700133.
 31. Shang, H., Zuo, Z., Li, L., Wang, F., Liu, H., Li, Y., and Li, Y. (2018). Ultrathin graphdiyne nanosheets grown in situ on copper nanowires and their performance as lithium-ion battery anodes. *Angew. Chem. Int. Ed. Engl.* **57**, 774–778.
 32. Li, G.X., Li, Y.L., Qian, X.M., Liu, H.B., Lin, H.W., Chen, N., and Li, Y.J. (2011). Construction of tubular molecule aggregations of graphdiyne for highly efficient field emission. *J. Phys. Chem. C* **115**, 2611–2615.
 33. Li, J.Q., Xu, J., Xie, Z.Q., Gao, X., Zhou, J.Y., Xiong, Y., Chen, C.G., Zhang, J., and Liu, Z.F. (2018). Diatomite-templated synthesis of freestanding 3D graphdiyne for energy storage and catalysis application. *Adv. Mater.* **30**, e1800548.
 34. Zhou, J.Y., Li, J.Q., Liu, Z.F., and Zhang, J. (2019). Exploring approaches for the synthesis of few-layered graphdiyne. *Adv. Mater.* **31**, e1803758.
 35. Gao, X., Liu, H., Wang, D., and Zhang, J. (2019). Graphdiyne: synthesis, properties, and applications. *Chem. Soc. Rev.* **48**, 908–936.
 36. Li, Y., Xu, L., Liu, H., and Li, Y. (2014). Graphdiyne and graphyne: from theoretical predictions to practical construction. *Chem. Soc. Rev.* **43**, 2572–2586.
 37. Sakamoto, J., van Heijst, J., Lukin, O., and Schlüter, A.D. (2009). Two-dimensional polymers: just a dream of synthetic chemists? *Angew. Chem. Int. Ed. Engl.* **48**, 1030–1069.
 38. Li, X., Zhang, H., and Chi, L. (2019). On-surface synthesis of Graphyne-based nanostructures. *Adv. Mater.* **31**, e1804087.
 39. Yu, H., Xue, Y., and Li, Y. (2019). Graphdiyne and its assembly architectures: synthesis, functionalization, and applications. *Adv. Mater.* **31**, e1803101.
 40. Sakamoto, R., Fukui, N., Maeda, H., Matsuoka, R., Toyoda, R., and Nishihara, H. (2019). The accelerating world of Graphdienes. *Adv. Mater.* **31**, e1804211.
 41. Haley, M.M., Bell, M.L., English, J.J., Johnson, C.A., and Weakley, T.J.R. (1997). Versatile synthetic route to and DSC analysis of Dehydrobenzoannulenes: crystal structure of a heretofore inaccessible [20] annulene derivative. *J. Am. Chem. Soc.* **119**, 2956–2957.
 42. Marsden, J.A., and Haley, M.M. (2005). Carbon networks based on dehydrobenzoannulenes. 5. Extension of two-dimensional conjugation in graphdiyne nanoarchitectures. *J. Org. Chem.* **70**, 10213–10226.
 43. Sonogashira, K., Tohda, Y., and Hagihara, N. (1975). A convenient synthesis of acetylenes: catalytic substitutions of acetylenic hydrogen with bromoalkenes, iodoarenes and bromopyridines. *Tetrahedron Lett.* **16**, 4467–4470.
 44. Diederich, F., and Rubin, Y. (1992). Synthetic approaches toward molecular and polymeric carbon allotropes. *Angew. Chem. Int. Ed. Engl.* **31**, 1101–1123.
 45. Glaser, C. (1869). Beiträge zur Kenntniss des Acetylnylbenzols. *Ber. Dtsch. Chem. Ges.* **2**, 422–424.
 46. Bohlmann, F.S.H., Schönowsky, H., Inhoffen, E., and Grau, G. (1964). Polyacetylenverbindungen, LII. über den Mechanismus der oxydativen Dimerisierung von Acetylenverbindungen. *Chem. Ber.* **97**, 794–800.
 47. Klappenberger, F., Zhang, Y.Q., Björk, J., Klyatskaya, S., Ruben, M., and Barth, J.V. (2015). On-surface synthesis of carbon-based scaffolds and nanomaterials using terminal alkynes. *Acc. Chem. Res.* **48**, 2140–2150.
 48. Li, Y.N., Wang, J.L., and He, L.N. (2011). Copper(II) chloride-catalyzed Glaser oxidative coupling reaction in polyethylene glycol. *Tetrahedron Lett.* **52**, 3485–3488.
 49. Wang, S.S., Liu, H.B., Kan, X.N., Wang, L., Chen, Y.H., Su, B., Li, Y.L., and Jiang, L. (2017). Superhydrophilicity-facilitated synthesis reaction at the microscale: ordered graphdiyne stripe arrays. *Small* **13**, 1602265.
 50. Hay, A.S. (1962). Oxidative coupling of acetylenes. II. *J. Org. Chem.* **27**, 3320–3321.
 51. Fomina, L., Vazquez, B., Tkatchouk, E., and Fomine, S. (2002). The Glaser reaction mechanism. A DFT study. *Tetrahedron* **58**, 6741–6747.
 52. Li, J., Gao, X., Li, Z.Z., Wang, J., Zhu, L., Yin, C., Wang, Y., Li, X.B., Liu, Z.F., Zhang, J., et al. (2019). Superhydrophilic graphdiyne accelerates interfacial mass/electron transportation to boost electrocatalytic and photoelectrocatalytic water oxidation activity. *Adv. Funct. Mater.* **29**, 1808079.
 53. Shang, H., Zuo, Z., Yu, L., Wang, F., He, F., and Li, Y. (2018). Low-temperature growth of all-carbon graphdiyne on a silicon anode for high-performance lithium-ion batteries. *Adv. Mater.* **30**, e1801459.
 54. Guo, S., Yan, H., Wu, F., Zhao, L., Yu, P., Liu, H., Li, Y., and Mao, L. (2017). Graphdiyne as electrode material: tuning electronic state and surface chemistry for improved electrode reactivity. *Anal. Chem.* **89**, 13008–13015.
 55. Guo, S., Yu, P., Li, W., Yi, Y., Wu, F., and Mao, L. (2020). Electron hopping by interfacing semiconducting graphdiyne nanosheets and redox molecules for selective electrocatalysis. *J. Am. Chem. Soc.* **142**, 2074–2082.
 56. Gao, X., Ren, H.Y., Zhou, J.Y., Du, R., Yin, C., Liu, R., Peng, H.L., Tong, L.M., Liu, Z.F., and

- Zhang, J. (2017). Synthesis of hierarchical Graphdiyne-based architecture for efficient solar steam generation. *Chem. Mater.* **29**, 5777–5781.
57. Gao, X., Zhou, J., Du, R., Xie, Z., Deng, S., Liu, R., Liu, Z., and Zhang, J. (2016). Robust superhydrophobic foam: A Graphdiyne-based hierarchical architecture for oil/water separation. *Adv. Mater.* **28**, 168–173.
58. Li, J.Q., Zhong, L.X., Tong, L.M., Yu, Y., Liu, Q., Zhang, S.C., Yin, C., Qiao, L., Li, S.Z., Si, R., and Zhang, J. (2019). Atomic Pd on Graphdiyne/Graphene heterostructure as efficient catalyst for aromatic nitroreduction. *Adv. Funct. Mater.* **29**, 1905423.
59. Eglinton, G., and Galbraith, A.R. (1956). Cyclic diynes. *Chemistry & Industry* **28**, 737–738.
60. Eglinton, G., and Galbraith, A.R. (1959). Macrocyclic acetylenic compounds. Part I. Cyclotetradeca-1,3-diyne and related compounds. *J. Chem. Soc.* **889**.
61. Klebansky, A.L., Grachev, I.V., and Kuznetsova, O.M. (1957). *J. Gen. Chem. USSR* **27**, 3008–3013.
62. Clifford, A.A., and Waters, W.A. (1963). 561. Oxidations of organic compounds by cupric salts. Part III. The oxidation of propargyl alcohol. *J. Chem. Soc.* **1963**, 3056–3062.
63. Ikegashira, K., Nishihara, Y., Hirabayashi, K., Mori, A., and Hiyama, T. (1997). Copper(I) salt promoted homo-coupling reaction of organosilanes 1997, 1039–1040.
64. Nishihara, Y., Ikegashira, K., Hirabayashi, K., Ando, J., Mori, A., and Hiyama, T. (2000). Coupling reactions of Alkynylsilanes mediated by a Cu(I) salt: novel syntheses of conjugate diynes and disubstituted ethynes. *J. Org. Chem.* **65**, 1780–1787.
65. Zhu, B.C., and Jiang, X.Z. (2007). A new CuAl-hydroxalcite catalyzed homocoupling reaction of terminal alkynes at room temperature. *Appl. Organometal. Chem.* **21**, 345–349.
66. Lu, X.L., Zhang, Y.H., Luo, C.C., and Wang, Y.G. (2006). Efficient and recyclable reaction system for the homocoupling of terminal acetylenes. *Synth. Commun.* **36**, 2503–2511.
67. Yadav, J.S., Reddy, B.V.S., Reddy, K.B., Gayathri, K.U., and Prasad, A.R. (2003). Glaser oxidative coupling in ionic liquids: an improved synthesis of conjugated 1,3-diynes. *Tetrahedron Lett.* **44**, 6493–6496.
68. Li, J.H., and Jiang, H.F. (1999). Glaser coupling reaction in supercritical carbon dioxide. *Chem. Commun.* **1999**, 2369–2370.
69. Chen, S.N., Wu, W.Y., and Tsai, F.Y. (2009). Homocoupling reaction of terminal alkynes catalyzed by a reusable cationic 2,2'-bipyridyl palladium(II)/CuI system in water. *Green Chem.* **11**, 269–274.
70. Kijima, M., Ohmura, K., and Shirakawa, H. (1999). Electrochemical synthesis of free-standing polyacetylene film with copper catalyst. *Synth. Met.* **101**, 58.
71. Sharifi, A., Mirzaei, M., and Naimi-Jamal, M.R. (2002). Copper-catalysed oxidative homocoupling of terminal acetylenes on alumina assisted by microwave irradiation. *J. Chem. Res.* **2002**, 628–630.
72. Schmidt, R., Thorwirth, R., Szuppa, T., Stolle, A., Ondruschka, B., and Hopf, H. (2011). Fast, ligand- and solvent-free synthesis of 1,4-substituted buta-1,3-diynes by Cu-catalyzed homocoupling of terminal alkynes in a ball mill. *Chemistry* **17**, 8129–8138.
73. Diercks, R., Armstrong, J.C., Boese, R., and Vollhardt, K.P.C. (1997). Hexaethynylbenzene †. *Angew. Chem. Int. Ed. Engl.* **25**, 268–269.
74. Gao, H.Y., Wagner, H., Zhong, D., Franke, J.H., Studer, A., and Fuchs, H. (2013). Glaser coupling at metal surfaces. *Angew. Chem. Int. Ed. Engl.* **52**, 4024–4028.
75. Zhao, F., Wang, N., Zhang, M., Sapi, A., Yu, J., Li, X., Cui, W., Yang, Z., and Huang, C. (2018). In situ growth of graphdiyne on arbitrary substrates with a controlled-release method. *Chem. Commun. (Camb.)* **54**, 6004–6007.
76. Colson, J.W., Woll, A.R., Mukherjee, A., Levendorf, M.P., Spittler, E.L., Shields, V.B., Spencer, M.G., Park, J., and Dichtel, W.R. (2011). Oriented 2D covalent organic framework thin films on single-layer graphene. *Science* **332**, 228–231.
77. Kim, K., Santos, E.J., Lee, T.H., Nishi, Y., and Bao, Z. (2015). Epitaxially grown strained pentacene thin film on graphene membrane. *Small* **11**, 2037–2043.
78. Li, J.Q., Xie, Z.Q., Xiong, Y., Li, Z.Z., Huang, Q.X., Zhang, S.Q., Zhou, J.Y., Liu, R., Gao, X., Chen, C.G., et al. (2017). Architecture of β -Graphdiyne-containing thin film using modified Glaser-Hay coupling reaction for enhanced photocatalytic property of TiO₂. *Adv. Mater.* **29**, 1700421.
79. Zwaneveld, N.A., Pawlak, R., Abel, M., Catalin, D., Gimes, D., Bertin, D., and Porte, L. (2008). Organized formation of 2D extended covalent organic frameworks at surfaces. *J. Am. Chem. Soc.* **130**, 6678–6679.
80. Dmitriev, A., Spillmann, H., Lin, N., Barth, J.V., and Kern, K. (2003). Modular assembly of two-dimensional metal-organic coordination networks at a metal surface. *Angew. Chem. Int. Ed. Engl.* **42**, 2670–2673.
81. Takada, K., Sakamoto, R., Yi, S.T., Katagiri, S., Kambe, T., and Nishihara, H. (2015). Electrochromic bis(terpyridine)metal complex nanosheets. *J. Am. Chem. Soc.* **137**, 4681–4689.
82. Rodenas, T., Luz, I., Prieto, G., Seoane, B., Miro, H., Corma, A., Kapteijn, F., Llabres I Xamena, F.X., and Gascon, J. (2015). Metal-organic framework nanosheets in polymer composite materials for gas separation. *Nat. Mater.* **14**, 48–55.
83. Sakamoto, R., Hoshiko, K., Liu, Q., Yagi, T., Nagayama, T., Kusaka, S., Tsuchiya, M., Kitagawa, Y., Wong, W.Y., and Nishihara, H. (2015). A photofunctional bottom-up bis(dipyrrinato)zinc(II) complex nanosheet. *Nat. Commun.* **6**, 6713.
84. Makiura, R., Motoyama, S., Umemura, Y., Yamanaka, H., Sakata, O., and Kitagawa, H. (2010). Surface nano-architecture of a metal-organic framework. *Nat. Mater.* **9**, 565–571.
85. Dai, W., Shao, F., Szczerbiński, J., McCaffrey, R., Zenobi, R., Jin, Y., Schlüter, A.D., and Zhang, W. (2016). Synthesis of a two-dimensional covalent organic monolayer through dynamic imine chemistry at the air/water interface. *Angew. Chem. Int. Ed. Engl.* **55**, 213–217.
86. Bauer, T., Zheng, Z., Renn, A., Enning, R., Stemmer, A., Sakamoto, J., and Schlüter, A.D. (2011). Synthesis of free-standing, monolayered organometallic sheets at the air/water interface. *Angew. Chem. Int. Ed. Engl.* **50**, 7879–7884.
87. Li, W.H., Liu, J., Yu, Y.X., Feng, G.Y., Song, Y., Liang, Q., Liu, L., Lei, S.B., and Hu, W.P. (2020). Synthesis of large-area ultrathin graphdiyne films at an air–water interface and their application in memristors. *Mater. Chem. Front.* **4**, 1268–1273.
88. Xue, Y.R., Guo, Y., Yi, Y.P., Li, Y.J., Liu, H.B., Li, D., Yang, W.S., and Li, Y.L. (2016). Self-catalyzed growth of Cu@graphdiyne core-shell nanowires array for high efficient hydrogen evolution cathode. *Nano Energy* **30**, 858–866.
89. Lv, J.X., Zhang, Z.M., Wang, J., Lu, X.L., Zhang, W., and Lu, T.B. (2019). In situ synthesis of CdS/graphdiyne heterojunction for enhanced photocatalytic activity of hydrogen production. *ACS Appl. Mater. Interfaces* **11**, 2655–2661.
90. Zuo, Z., Shang, H., Chen, Y., Li, J., Liu, H., Li, Y., and Li, Y. (2017). A facile approach for graphdiyne preparation under atmosphere for an advanced battery anode. *Chem. Commun. (Camb.)* **53**, 8074–8077.